Rotational energy relaxation of individual rotational states in liquids

Joonkyung Jang, and Richard M. Stratt

Citation: The Journal of Chemical Physics **113**, 5901 (2000);
View online: https://doi.org/10.1063/1.1290289
View Table of Contents: http://aip.scitation.org/toc/jcp/113/14
Published by the American Institute of Physics

Rotational energy relaxation of individual rotational states in liquids

Joonkyung Jang and Richard M. Stratt[a)]
Department of Chemistry, Brown University, Providence, Rhode Island 02912

(Received 8 June 2000; accepted 11 July 2000)

The manner in which most molecules reorient in liquids bears little resemblance to the process in the gas phase. For small-moment-of-inertia species such as the hydrides, however, the observation of discrete spectroscopic lines corresponding to individual isolated-molecule quantum transitions suggests that one is actually seeing single-molecule dynamics perturbed only weakly by the environment—just as one sees with solution-phase vibrational behavior. We examine here the degree to which such individual rotational quantum states remain well defined in liquids by considering the rates of discrete energy-level-to-energy-level transitions in solution. For rotational quantum states that do preserve their free-rotor character in a liquid, we find that the transition rate between angular momentum states obeys a rotational Landau–Teller relation strikingly similar to the analogous expression for vibration: the rate is proportional to the liquid's rotational friction evaluated at the transition frequency. Subsequent evaluation of this friction by classical linearized instantaneous-normal-mode theory suggests that we can understand this relationship by regarding the relaxation as a kind of resonant energy transfer between the solute and the solution modes. On specializing to the particular cases of H_2 and D_2 in $Ar_{(l)}$, we find that the most critical modes are those that move the light solute's center of mass with respect to a single nearby solvent. This observation, in turn, suggests a generalization of instantaneous-normal-mode ideas that transcends both linear coupling and harmonic dynamics: an instantaneous-pair theory for the relaxation of higher-lying levels. By employing a linearized instantaneous-normal-mode theory of relaxation within the liquid band and an instantaneous-pair theory for higher-frequency relaxation, we find that the resonant-transfer paradigm is reasonably successful in reproducing molecular dynamics results spanning a wide range of different rotational states. © *2000 American Institute of Physics.* [S0021-9606(00)50138-X]

I. INTRODUCTION

There are comparatively few examples of molecules whose discrete rotational quantum states survive immersion in a liquid. The isolated-molecule energy level spacings are not only typically far smaller than the thermal energy, the violent torques exerted by a solvent make for relaxation rates rapid compared to rotational periods. The end result is that straightforward spectroscopic measurements of reorientational dynamics in liquids will rarely see anything besides some sort of generic rotational diffusion. Most fluorescence depolarization experiments, in particular, tend to provide little in the way of microscopic insight into the processes by which rotations come to equilibrium in liquids. It is not that the values of the diffusion constants obtained from such experiments do not carry any molecular information; recent studies have emphasized that simple theories portraying the solute as a featureless sphere (or ellipsoid) in a homogenized continuum will not always work,[1] and even when they do, they may need a fairly careful representation of the solute charge distribution to do them justice.[2] What we can say, though, is that the potentially interesting mechanical details of the solvent *dynamics* are invariably obscured by diffusional motion.

The molecules that do fall into the select category of exhibiting quantized rotation in liquids, however, offer us an intriguing spectroscopic window into how gas-phase quantum dynamics can be altered by a liquid environment.[3–15] To a certain extent, this same information is revealed by experiments that follow the rotational behavior of gases as a function of increasing density.[16] But, unless the separate spectroscopic lines from individual rotational states persist into the liquid phase, these studies run out of information just when they reach the regime we would like to understand.[5]

The solutes we would like to focus on here are the hydrides, the molecules with the smallest moments of inertia, and thus the largest rotational energy level spacings: H_2, D_2, and HCl, for example.[3–14] It has been known for quite some time that solutions of dihydrogen,[9–11,13,14] the hydrogen-halides,[3–8] and ammonia[6] (and their deuterium substituted analogues) all exhibit clear remnants of gas-phase rotational energy levels in their infrared (IR), far-IR, or rotational Raman spectra, at least under certain conditions. In fact, part of the motivation of this work is the recent attention devoted to the spectroscopy of solutions of H_2 and D_2.[9–14] State resolved rotational-Raman spectra of these species have now been measured in supercritical CO_2,[9] and in both liquid and solid H_2O.[10,11,14] Yet the details of the earlier studies, the line shapes and even the conditions under which one should expect to see discrete spectral lines, remain poorly understood. The first far-IR studies of HCl and DCl in $SF_{6(l)}$ displayed well-resolved peaks for the $J \rightarrow J+1$ HCl

a)Electronic mail: richard_stratt@brown.edu

rotational transitions,[3] but only the rotational Raman spectrum (looking at $J \rightarrow J+2$ transitions) shows the corresponding peaks for DCl.[8] Far IR studies of HCl in the noble gases are similarly striking.[5] Individual rotational lines become progressively better resolved as one proceeds from $Ar_{(l)}$ to $Kr_{(l)}$ to $Xe_{(l)}$ solvents—exactly opposite from what one might expect from general tendency of increasing solute–solvent interaction to broaden spectral lines. Some of this trend is undoubtedly a result of the fact that the three noble-gas solvents have been studied at successively higher temperatures (thereby increasing the intensity of the more easily resolved higher frequency lines). Still, when one looks just at the more comparable lower–frequency transitions, the basic counterintuitive trend seems to remain.[6]

Theoretical efforts at understanding rotational energy relaxation have been neither plentiful nor targeted at quantum-state-resolved systems. There have been a few interesting molecular dynamics studies of classical rotational energy autocorrelation functions in liquids,[17–19] but not nearly as many as there have been of orientational and angular-velocity autocorrelation functions. Similarly there have been efforts at predicting the rotational and rovibrational spectroscopy of hydride solutions, but based on phenomenological rather than microscopic treatments of the solvent.[20] The papers closest in spirit to the present work are the groundbreaking fully microscopic, mixed-quantum-classical simulations of rotational Raman spectrum of H_2 in $H_2O_{(l,s)}$ and in $Ar_{(l)}$,[13,14] but here as well, energy transfer *per se* was not the focus. Indeed in the case of $Ar_{(l)}$, no transitions between J levels seemed to be necessary to account for the spectra.[13]

The goal of this article will not be to rationalize the rotational spectroscopy of dissolved hydrides. We defer such specific spectroscopic predictions to a future article.[21] What we would like to do instead is to look at the more fundamental issue, the length of time a rotational quantum state can maintain its identity in a liquid. In particular, we would like to understand the rate at which rotational energy relaxes—the rate at which a liquid induces inelastic angular-momentum-state to angular-momentum-state quantum transitions. There has never been a direct measurement of such rotational energy lifetimes (T_1 values) in the liquid-state, so a quantitative prediction might be of some use in its own right. More to the point, though, seeing the way that these well-defined quantum mechanical energy levels (with spacings on the order of hundreds of cm^{-1}) manage to persist in a liquid makes it natural to wonder about the parallels between the fates of rotational and vibrational states in liquids. Will the time scales and molecular mechanisms relevant to rotational population relaxation have any resemblance to those seen in the much more familiar case of vibrational population relaxation?[22,23]

As is well known, the basic phenomenology of vibrational population relaxation rates in liquids is described rather accurately by Landau–Teller theory, a result easily understood as a straightforward application of Fermi's golden rule.[22,24,25] A harmonic vibration with frequency ω_0 and reduced mass μ is predicted to undergo a transition from quantum state n to quantum state $n-1$ with a rate

$$k_{n\rightarrow n-1} = (2n/\mu\hbar\omega_0\beta)[1+\exp(-\hbar\omega_0\beta)]^{-1}\hat{\eta}_{\mathrm{vib}}(\omega_0). \tag{1.1}$$

The factor in the brackets is needed to build in the detailed-balance condition that at a temperature T [with $\beta = 1/(k_B T)$]

$$k_{n\rightarrow n-1}/k_{n-1\rightarrow n} = \exp(\hbar\omega_0\beta), \tag{1.2}$$

but the details of the energy transfer process itself appear in the *vibrational friction* $\hat{\eta}_{\mathrm{vib}}(\omega)$, which (at the level of this development) is simply the cosine transform of a force autocorrelation function

$$\hat{\eta}_{\mathrm{vib}}(\omega) = \int_0^\infty dt \cos\omega t\, \eta_{\mathrm{vib}}(t), \tag{1.3a}$$

$$\eta_{\mathrm{vib}}(t) = \beta\langle F(t)F(0)\rangle, \tag{1.3b}$$

with the force F what the force exerted by the solvent along the normal mode coordinate would be if the normal coordinate were held fixed.[26–28]

In the generalized-Langevin-equation formulation of vibrational dynamics, this correlation function actually is a ''friction'' in the very literal sense that the drag force on the vibrating coordinate stems from the convolution of this friction with the velocity.[27,28] [Technically, what is called for is the autocorrelation function of a force ''dynamically orthogonal'' to the vibration, but the distinction seems to be unimportant in practice.[28]] Thus Eq. (1.1) has a nice interpretation as a statement of the fluctuation-dissipation theorem[29]—that the (nonequilibrium) rate at which quanta of vibrational energy $\hbar\omega_0$ are dissipated into the solvent is proportional to the magnitude of the solvent's own (equilibrium) fluctuations at frequency ω_0. But what of rotational relaxation? Though it seems not to have been widely applied, the generality of this result suggests that there should be an analogous principle for rotational dynamics. One of the goals of this article is to show that a fluctuation-dissipation relationship of precisely this sort does indeed govern the rate of rotational energy relaxation and that we can therefore understand the molecular mechanisms behind this quantum mechanical relaxation by delving into the microscopics of the classical rotational friction. To be specific, at the same level of approximation used in defining the vibrational friction, this rotational friction $\hat{\eta}_{\mathrm{rot}}(\omega)$ is

$$\hat{\eta}_{\mathrm{rot}}(\omega) = \int_0^\infty dt \cos\omega t\, \eta_{\mathrm{rot}}(t), \tag{1.4a}$$

$$\eta_{\mathrm{rot}}(t) = (1/2)\beta\langle \mathbf{N}(t)\cdot\mathbf{N}(0)\rangle, \tag{1.4b}$$

where $\mathbf{N}$ is the torque exerted by the solvent on a solute whose orientation is held fixed,[30–32] so we shall first need to make a connection between the quantum mechanical rotational–state to rotational–state transition rate and this quantum mechanical torque autocorrelation function. We then need to find a route—in practice a classical mechanical route—to computing and analyzing this correlation function.

Aiding us considerably in this endeavor is the fact that it is possible to understand rotational[31,32] (and vibrational)[33–37] friction in terms of the instantaneous normal modes (INMs) of the liquid.[38,39] The INM perspective is that the complicated collective dynamics of the solution can be resolved

into microscopically well-defined contributions from harmonic modes spanning the natural frequency range of the liquid (its ''band''). It turns out that not only are frequency-domain frictions given reasonably accurately in such a formulation, but the molecular definitions of the modes allow for a facile analysis of the principal mechanical motions that lead to relaxation.[23,33,35–37] Moreover, the very notion of a band will help us make some interesting distinctions between the microscopic mechanisms appropriate to rotational transitions inside and outside of the band.

The remainder of this article will be organized as follows: In Sec. II we develop a perturbation theory suitable for treating rotational energy–level to energy–level transitions for the just kinds of liquid solutions that allow for discrete solute rotational levels. The resulting rate is then connected, at the same level of perturbation theory, to the rotational friction resolved into separate contributions from each order of anisotropy in the solute–solvent interaction. Section III presents both our linearized INM theory and an instantaneous-pair theory for this anisotropy-resolved friction, the former for evaluating the friction at frequencies within the INM band and the latter (in both dynamically exact and nonlinear INM versions) for frequencies beyond the band edge. The models and calculational details for our numerical case studies of H_2 and D_2 in $Ar_{(l)}$ are described in Sec. IV and in Sec. V we present the numerical results we obtained by applying our formalism to these examples. We conclude in Sec. VI with some comments on possible connections with spectroscopic observables.

II. ROTATIONAL ENERGY RELAXATION RATES AND ROTATIONAL FRICTION

A. Perturbative treatment of level-to-level rotational energy relaxation in liquids

Consider a single linear, rigid-rotor solute dissolved in an atomic liquid. The key dynamical variables of interest are the angles θ and ϕ specifying the solute orientation in the laboratory frame, so we shall take the remaining degrees of freedom, the center-of-mass position of the solute, $\mathbf{r}_0$, and the location of the N solvent atoms $\mathbf{R}=(\mathbf{r}_1,\ldots,\mathbf{r}_N)$, to make up our bath. The total Hamiltonian can thus be divided into portions corresponding to solute rotation, $H_{\rm rot}$, bath translation, H_B, and whatever anisotropic interaction there may be between the solute and the solvent, V,

$$H=H_{\rm rot}(\theta,\phi,\dot{\theta},\dot{\phi})+H_B(\dot{\mathbf{R}},\mathbf{R})+V(\theta,\phi,\mathbf{R}). \tag{2.1}$$

We are only interested in situations in which the anisotropic interaction is sufficiently weak and slowly varying that individual rotational states remain reasonably well defined even when the rotor is dissolved. We can therefore safely expand this interaction in spherical harmonics $Y_{JM}(\theta,\phi)$

$$V(\theta,\phi,\mathbf{R})=\sum_{J=1}^{\infty}\sum_{M=-J}^{J}A_{JM}(\mathbf{R})Y_{JM}(\theta,\phi), \tag{2.2}$$

with expansion coefficients

$$A_{JM}(\mathbf{R})=\int_0^{2\pi}d\phi\int_0^{\pi}d\theta\sin\theta\; Y^*_{JM}(\theta,\phi)V(\theta,\phi,\mathbf{R}). \tag{2.3}$$

Note that the bath Hamiltonian contains the isotropic ($J=0$) portion of the solute–solvent interaction—which, in general, will be neither weak nor slowly varying. However, it is the anisotropy of the bath, the $A_{JM}(\mathbf{R})$ coefficients ($J\geqslant 1$), whose dynamics will turn out to matter.

In the absence of any solvent-induced anisotropy, the solute would reside in a free-rotor quantum state $|lm\rangle$,

$$H_{\rm rot}|lm\rangle=E_l|lm\rangle,\quad E_l=(\hbar^2/2I)l(l+1), \tag{2.4}$$

with l and m the quantum numbers prescribing the total angular momentum and its laboratory-frame z-axis projection, and I the solute moment of inertia. In order to ensure that the solvent effects are weak enough to keep l and m as good quantum numbers, we will presumably want the average off-diagonal (l,l') matrix elements of the anisotropic interaction to be small compared to the corresponding (l,l') energy level spacings. That is we shall look for

$$\langle V^2_{ll'}\rangle\ll|E_l-E_{l'}|^2, \tag{2.5a}$$

$$V^2_{ll'}(\mathbf{R})\equiv(2l+1)^{-1}(2l'+1)^{-1}\times\sum_{m=-l}^{l}\sum_{m'=-l'}^{l'}|V_{lm,l'm'}(\mathbf{R})|^2, \tag{2.5b}$$

$$V_{lm,l'm'}(\mathbf{R})\equiv\langle lm|V|l'm'\rangle, \tag{2.5c}$$

where the brackets in Eq. (2.5a) refer to a classical ensemble average over the liquid configurations $\mathbf{R}$. Though this condition would typically *not* be satisfied for most molecules in liquids,[40] the tiny moments of inertia and nearly spherical interactions found with H_2 and D_2 will, in fact, allow us to satisfy this condition comfortably.

Assuming then, that Eq. (2.5a) holds, we can define the desired $l\rightarrow l'$ rate constant as the sum over all final, and average over all initial, m states.

$$k_{l\rightarrow l'}=(2l+1)^{-1}\sum_{m=-l}^{l}\sum_{m'=-l'}^{l'}k_{lm\rightarrow l'm'}, \tag{2.6}$$

and then calculate it, at least in principle, via Fermi's golden rule,

$$k_{lm\rightarrow l'm'}=(2\pi/\hbar)\sum_{a,b}P_a|\langle a|V_{lm,l'm'}(\mathbf{R})|b\rangle|^2\times\delta(E_l-E_{l'}+E_a-E_b). \tag{2.7}$$

Here $|a\rangle$ and $|b\rangle$ are eigenstates of the bath Hamiltonian H_B, and P_a is the equilibrium probability of the bath being in the ath state. Moreover since Eq. (2.2) tells us that

$$V_{lm,l'm'}(\mathbf{R})=\sum_{J=1}^{\infty}\sum_{M=-J}^{J}A_{JM}(\mathbf{R})\langle lm|Y_{JM}|l'm'\rangle,$$

it is possible to rewrite the rate constant in terms of time correlation functions of the anisotropy coefficients

$$k_{l\to l'}=\hbar^{-2}(2l+1)^{-1}\sum_m\sum_{m'}\sum_{JM}\sum_{J'M'}\langle lm|Y_{JM}|l'm'\rangle \times\langle lm|Y_{J'M'}|l'm'\rangle\int_{-\infty}^{\infty}dt\,\exp(i\Omega_{ll'}t) \times\langle A_{JM}(t)A^*_{J'M'}(0)\rangle, \tag{2.8}$$

much as in the analogous problem of vibrational relaxation in liquids. The quantity $\Omega_{ll'}$ here refers to the transition frequency

$$\Omega_{ll'}=(E_l-E_{l'})/\hbar, \tag{2.9}$$

and by expressions such as $A(t)$ we mean the time evolution following the hypothetical pure bath (completely isotropic) dynamics

$$A_{JM}(t)=\exp(iH_Bt/\hbar)A_{JM}(\mathbf{R})\exp(-iH_Bt/\hbar). \tag{2.10}$$

Not surprisingly, the fact that liquids are isotropic on the average allows us to simplify these expressions considerably. In particular, time correlation functions of the form appearing in Eq. (2.8) must not only be diagonal in both J and M, but independent of M[11]

$$\langle A_{JM}(t)A^*_{J'M'}(0)\rangle=\delta_{JJ'}\delta_{MM'}\langle A_{J0}(t)A_{J0}(0)\rangle, \tag{2.11}$$

meaning that

$$k_{l\to l'}=\hbar^{-2}(2l+1)^{-1}\sum_J\sum_{m,m'}\sum_M\langle lm|Y_{JM}|l'm'\rangle^2 \times\int_{-\infty}^{\infty}dt\,\exp(i\Omega_{ll'}t)\langle A_{J0}(t)A_{J0}(0)\rangle$$

or, in terms of standard $3-j$ symbols,[41]

$$k_{l\to l'}=\hbar^{-2}\int_{-\infty}^{\infty}dt\,\exp(i\Omega_{ll'}t)\sum_J b_JF_{ll'}(J) \times\langle A_{J0}(t)A_{J0}(0)\rangle, \tag{2.12}$$

$$F_{ll'}(J)\equiv\frac{(2l'+1)}{J(J+1)}\begin{pmatrix} l & J & l' \\ 0 & 0 & 0\end{pmatrix}^2, \qquad b_J\equiv J(J+1)(2J+1)/4\pi. \tag{2.13}$$

Equation (2.12) is as much as we can say quantum mechanically about our rate constants. However, for most solvents we might be interested in (superfluid He being an intriguing exception),[15] we might expect the dynamics of our bath to be rather classical. It therefore makes sense to pursue some sort of classical or semiclassical approximation to the quantum mechanical bath correlation function that lies at the heart of Eq. (2.12). How best to do so has been a subject much discussed in the literature of late.[42,43] Depending on which particular features of the quantum problem need to be preserved (the correct short-time limits, say, or the exact behavior in some special case or other), there are a variety of plausible routes, all of which allow us to compute the correlation function classically and use the result to estimate the quantum correlation function.[42–46] Regardless of which avenue we pursue though, we shall need to ensure quantum mechanically correct detailed balance,

$$k_{l\to l'}/k_{l'\to l}=[(2l'+1)/(2l+1)]\exp(\hbar\Omega_{ll'}\beta), \tag{2.14}$$

where the prefactor arises from the ratios of the number of m states associated with the two energy levels—and to do so we shall need to preserve the proper time reversal invariance

$$\int_{-\infty}^{\infty}dte^{i\Omega t}\langle A_{J0}(-t)A_{J0}(0)\rangle =\exp(-\hbar\Omega\beta)\int_{-\infty}^{\infty}dte^{i\Omega t}\langle A_{J0}(t)A_{J0}(0)\rangle,$$

where $\beta=(k_BT)^{-1}$ with k_B Boltzmann's constant and T the temperature.[47]

The approach we shall take here to satisfy these conditions is to use the technique, familiar in studies of vibrational relaxation, of expressing the quantal correlation function in terms of its real part, and identifying that real part with the classical equivalent.[25] Since for any quantum mechanical correlation function $C(t)$, $C(-t)=C^*(t)$[47]

$$\int_{-\infty}^{\infty}dte^{i\Omega t}\langle A_{J0}(t)A_{J0}(0)\rangle =2(1+e^{-\hbar\Omega\beta})^{-1}\int_{-\infty}^{\infty}dte^{i\Omega t}\,\mathrm{Re}[\langle A_{J0}(t)A_{J0}(0)\rangle] \approx2(1+e^{-\hbar\Omega\beta})^{-1}\int_{-\infty}^{\infty}dte^{i\Omega t}C_J(t),$$

where $C_J(t)$ is the *classical* time correlation function for the Jth order anisotropy coefficient

$$C_J(t)=\langle A_{J0}(t)A_{J0}(0)\rangle. \tag{2.15}$$

Substituting this approximation into Eq. (2.12) yields our basic semiclassical approximation to the level-to-level transition rate

$$k_{l\to l'}=4\hbar^{-2}[1+\exp(-\hbar\Omega_{ll'}\beta)]^{-1} \times\sum_{J=1}^{\infty}b_JF_{ll'}(J)\hat{C}_J(\Omega_{ll'}). \tag{2.16}$$

Here $\hat{C}_J(\omega)$ is the cosine transform of our anisotropy correlation function

$$\hat{C}_J(\omega)=\int_0^{\infty}dt\cos\omega tC_J(t). \tag{2.17}$$

Notice that by interchanging l and l' in Eqs. (2.16) and (2.13) one can show that we do indeed satisfy Eq. (2.14), the detailed balance condition.

B. The role of friction in rotational energy relaxation

The anisotropy correlation functions may seem to be rather abstruse quantities, but they are related rather simply to the torque autocorrelation function—which, in turn, sets the rotational friction felt by our solute. To see this connection, consider the spherical harmonic expansion of the torque on the solute. From Eq. (2.2)

$$N_z=-\partial V/\partial\phi=i\sum_{JM}MA_{JM}(\mathbf{R})Y_{JM}(\theta,\phi).$$

Taking the rotor angles to be fixed at their initial values θ_0 and ϕ_0 for the duration of the friction dynamics then yields the correlation function we need for the friction

$$\langle \mathbf{N}(t)\cdot\mathbf{N}(0)\rangle_{\text{frozen-orientation}} = 3\langle N_z(t)N_z(0)\rangle_{\text{frozen-orientation}} = 3\sum_{JM}\sum_{J'M'} MM'\langle A_{JM}(t)A^*_{J'M'}(0)Y_{JM}(\theta_0,\phi_0) \times Y^*_{J'M'}(\theta_0,\phi_0)\rangle,$$

where the average is over all of the initial conditions.

Suppose, consistent with the weak anisotropy assumptions of Sec. II A, we now assume that the dynamics of the solvent anisotropy coefficients $A_{JM}(t)$ are uncorrelated with the solute orientation

$$\langle \mathbf{N}(t)\cdot\mathbf{N}(0)\rangle_{\text{frozen-orientation}} \approx 3\sum_{JM}\sum_{J'M'} MM'\langle A_{JM}(t)A^*_{J'M'}(0)\rangle \times\langle Y_{JM}(\theta_0,\phi_0)Y^*_{J'M'}(\theta_0,\phi_0)\rangle.$$

Since $\langle Y_{JM}Y^*_{J'M'}\rangle = (4\pi)^{-1}\delta_{JJ'}\delta_{MM'}$, the isotropy of the liquid, Eq. (2.11), lets us express our results in terms of the anisotropy correlation functions, Eq. (2.15)

$$\langle \mathbf{N}(t)\cdot\mathbf{N}(0)\rangle_{\text{frozen-orientation}} = \sum_{J=1}^{\infty}\langle \mathbf{N}(t)\cdot\mathbf{N}(0)\rangle_J, \quad (2.18a)$$

$$\langle \mathbf{N}(t)\cdot\mathbf{N}(0)\rangle_J = b_J C_J(t). \quad (2.18b)$$

Thus the friction, Eq. (1.4b), can be written in this same limit as a sum over these correlation functions

$$\eta(t) = \sum_{J=1}^{\infty}\eta_J(t), \quad (2.19a)$$

$$\eta_J(t) \equiv (b_J/2k_BT)C_J(t). \quad (2.19b)$$

Our semiclassical approximation to the rotational energy relaxation rate, Eq. (2.16), therefore takes the simple form

$$k_{l\to l'} = 8k_BT\hbar^{-2}[1+\exp(-\hbar\Omega_{ll'}\beta)]^{-1} \times\sum_{J=1}^{\infty}F_{ll'}(J)\,\hat{\eta}_J(\Omega_{ll'}), \quad (2.20)$$

where the angular-momentum coupling coefficients $F_{ll'}(J)$ are defined by Eq. (2.13) and the frequency-domain frictions are just cosine transforms

$$\hat{\eta}_J(\omega) = \int_0^{\infty} dt\cos\omega t\,\eta_J(t). \quad (2.21)$$

Equation (2.20) is the principal result of this article. It points out that in order for our solute to be able to switch from one rotational level l to another l', the solvent must be able to generate rotational friction at a frequency $\Omega_{ll'}$ given by Eq. (2.9). The angular momentum considerations inherent in Eq. (2.13), moreover, impose the selection rule that a new level l' is only accessible from l through a Jth order friction if[41(b)]

$$l+l'+J = \text{even}, \quad 1 \leqslant |l-l'| \leqslant J. \quad (2.22)$$

For the particular case we treat in this article, that of H_2 in Ar, the situation is even simpler than this general framework describes. Our anisotropic solute–solvent interaction only includes a single J term ($J=2$), meaning that there is only a single term, that for $J=2$ in Eqs. (2.19a) and (2.20). The rotational relaxation rate is thus literally proportional to the total frequency domain friction

$$k_{l\to l'} = 8k_BT\hbar^{-2}[1+\exp(-\hbar\Omega_{ll'}\beta)]^{-1}F_{ll'}(2)\,\hat{\eta}(\Omega_{ll'}), \quad (2.23)$$

the precise analogue of the Landau–Teller formula for vibrational energy relaxation.[22,24–26]

Interestingly, these same expressions allow us to give a nice classical interpretation of Eq. (2.5), our quantum mechanical criterion for the validity of our weak anisotropy treatment. From Eqs. (2.2), (2.5b), (2.5c), and (2.13), and the liquid isotropy condition Eq. (2.11), we know that the mean-square off-diagonal matrix element is given by

$$\langle V^2_{ll'}\rangle = (2l'+1)^{-1}\sum_{J=1}^{\infty} b_J F_{ll'}(J)\langle A^2_{J0}(0)\rangle.$$

However, Eqs. (2.15) and (2.18) tell us that the average on the right-hand side is basically the Jth component of the mean-square torque. Hence we can write

$$\langle V^2_{ll'}\rangle = \sum_{J=1}^{\infty} K_{ll'}(J)\langle \mathbf{N}^2(0)\rangle_J, \quad (2.24)$$

with

$$K_{ll'}(J) = (2l'+1)^{-1}F_{ll'}(J) = [J(J+1)]^{-1}\begin{pmatrix} l & J & l' \\ 0 & 0 & 0\end{pmatrix}^2. \quad (2.25)$$

For H_2 in Ar, then, it is clear that our perturbative analysis will be valid when the mean-square torque is small compared to the energy level spacing,

$$\langle \mathbf{N}^2(0)\rangle \ll |E_l - E_{l'}|^2/K_{ll'}(2). \quad (2.26)$$

This finding is, in fact, the quantum mechanical analogue of the observation commonly made in interpreting rotational behavior in liquids: ''strong-torque'' liquids lead to a relatively fast onset of diffusive rotational motion whereas ''weak-torque'' liquids have a more free-rotor, inertial, character to their rotational dynamics.[48]

III. INSTANTANEOUS-NORMAL-MODE AND INSTANTANEOUS-PAIR THEORIES FOR ROTATIONAL FRICTION

A. Instantaneous-normal-mode theory for rotational friction: Linear theory

Now that we have a Landau–Teller-like theory connecting rotational energy relaxation to rotational friction, it is clear that we can explore energy relaxation processes by examining the molecular origins of the frequency-domain friction. We can certainly obtain accurate numerical values for this friction (at least for modest frequencies) through a molecular dynamics evaluation of the torque autocorrelation

function, Eq. (1.4).[30,31] However, besides simply carrying out such calculations, we would like to deepen our qualitative understanding by finding out which specific kinds of molecular motion are associated with the relaxation of each rotational level.

One of the more useful routes for pursuing this kind of analysis makes use of an instantaneous-normal-mode (INM) treatment of the friction. INM theories for vibrational[33–37] and rotational[31,32] friction have proven to be reasonably successful in this regard, producing values for the frequency-domain friction respectably close to those computed from molecular dynamics and allowing facile partitioning of the friction into easily interpretable microscopic components. The rotational friction we need here is actually a little different from that computed previously[31,32] in that it has to be resolved into separate contributions from each order of anisotropy. Still, the derivation is sufficiently close to our previous work that we limit ourselves to a brief summary of the development.

The basic INM idea is that, for short times, the time evolution of a liquid from an initial configuration $\mathbf{R}_0$ to some configuration $\mathbf{R}_t$ at time t can be described by a set of collective harmonic modes, the INMs.[49]

$$q_\alpha(t)=\sum_{j\mu} U_{\alpha,j\mu} m_j^{1/2}[r_{j\mu}(t)-r_{j\mu}(0)];$$
$$\alpha=1,...,3(N+1). \tag{3.1}$$

Here $r_{j\mu}$ is the μth Cartesian component ($\mu=x,y,z$) of the position vector of the jth atom or independent site in the system. In our particular case, with a diatomic solute in an atomic solvent, we will want to allow for the collective motion involving not only the solvent atoms ($j=1,...,N$), but also the center of mass of the solute ($j=0$). The matrices $\boldsymbol{U}(\mathbf{R}_0)$ which define the modes are prescribed by the requirement that they diagonalize the so called dynamical matrix $\boldsymbol{D}(\mathbf{R}_0)$, the matrix of mass-weighted second derivatives of the potential energy. In terms of our Hamiltonian, Eq. (2.1),

$$[\boldsymbol{U}^T(\mathbf{R}_0)\boldsymbol{D}(\mathbf{R}_0)\boldsymbol{U}(\mathbf{R}_0)]_{\alpha\beta}=\omega_\alpha^2\delta_{\alpha\beta}, \tag{3.2}$$

$$D_{j\mu,kv}=(m_j m_k)^{-1/2}\partial^2 H_B/\partial r_{j\mu}\partial r_{kv}. \tag{3.3}$$

Since the dynamics of the modes themselves is harmonic we can evaluate time correlation functions just by writing the important dynamical variables in terms of them. In particular, we know from Eqs. (2.15) and (2.19) that we can compute the friction we need from the anisotropy correlation functions $C_J(t)$. The *linear INM theory* for the rotational friction then arises by assuming that displacements of the anisotropy coefficients are linear in the modes

$$A_{J0}(t)\approx A_{J0}(0)+\sum_\alpha (\partial A_{J0}/\partial q_\alpha)_{\mathbf{q}=\mathbf{0}}\, q_\alpha(t). \tag{3.4}$$

Substituting in the INM dynamics,[49] evaluating the second derivative of the $C_J(t)$ correlation functions, and cosine transforming the results yields our desired expression for the frequency-domain friction, Eq. (2.21).[50,51]

$$\hat{\eta}_J(\omega)=(\pi/2)\rho_J(\omega)/\omega^2. \tag{3.5}$$

The spectral densities $\rho_J(\omega)$ appearing here are the so-called influence spectra of the liquid, the spectra of INM modes weighted by coupling constants c_α^J reflecting the ability of each mode α to influence the Jth order anisotropy.

$$\rho_J(\omega)=\left\langle \sum_\alpha (c_\alpha^J)^2\delta(\omega-\omega_\alpha)\right\rangle,$$
$$c_\alpha^J=(b_J/2)^{1/2}(\partial A_{J0}/\partial q_\alpha)_{\mathbf{q}=\mathbf{0}}. \tag{3.6}$$

It is the fully molecular definition of such coupling constants that will allow us to project out the key molecular events in rotational energy relaxation.[32,33,36,37,52]

B. Instantaneous-pair theory and its nonlinear INM implementation

The physical picture suggested by this linear INM theory is that rotational energy relaxation occurs by a kind of resonant energy transfer; a quantum of rotational energy $\hbar\Omega$ can be lost to the solvent if it goes into a bath mode with the same frequency Ω. Indeed, our experience with vibrational energy relaxation (for which linear INM theory predicts precisely the same scenario)[23] suggests that this idea should be more or less quantitative. However, as with vibrational relaxation, we also know that this approach can only work when the transition frequencies lie within the INM band—within the natural frequency range of the liquid.[53] The problem is that once we get beyond the first few rotational states in H_2, we quickly cross the band ''edge.'' For the higher frequency transitions we would actually expect our Landau–Teller-like theory to fare rather poorly were we to insist on computing the friction from harmonic solvent modes selected from within the INM band.

When we were confronted with these same issues in studying high-frequency vibrational relaxation in liquids we noted that they did not necessarily invalidate the basic idea of liquid modes.[23,53] It was conceivable, for example, that the dominant relaxation pathway might continue to rely on bath modes, but that these modes might be significantly anharmonic. Alternatively, some suitable nonlinear coupling of a solute to an otherwise harmonic set of solvent modes might act to mimic the effects of anharmonic modes, a possibility widely appreciated in a solid-state context.[54] On exploring the matter in detail, what we found was that the actual mechanism of vibrational relaxation was extraordinarily simple, making it possible to test both of these alternatives—and to choose between them. To achieve frequencies well outside the INM band, the relevant dynamics has to be so local that it needs to reside almost entirely in the pair motion of the solute and the nearest solvent.[36,37,53] As a result, it is possible to formulate a fully anharmonic, fully nonlinearly coupled, treatment based on an *instantaneous-pair* perspective: each liquid configuration in which the solute and a solvent form what we called a mutual-nearest-neighbor pair[36,53,55] is regarded as an instantaneous starting point for a two-body, one-dimensional, classical trajectory involving just the solute and the special solvent. The friction correlation function (there, a force autocorrelation function) can then be evaluated by assuming that it is only the forces be-

tween the pair that drive the relevant dynamics and that all the dynamics does is make those intrapair forces evolve.[53]

Can the same kind of instantaneous-pair theory serve to explain high-frequency rotational energy relaxation? Presumably the same arguments we used to motivate the locality of the high frequency dynamics of *forces* should still apply when we switch to considering the *torques* on a solute. Consider, in particular, the velocity version of the friction, Eq. (2.19) with Eq. (2.15)[51]

$$\ddot{\eta}_J(t) = -(b_J/2k_BT)\langle \dot{A}_{J0}(t)\dot{A}_{J0}(0)\rangle. \tag{3.7}$$

The anisotropy coefficients, which are closely related to the torques, can be expressed as sums of solute–solvent pair contributions as long as the anisotropic potential itself, Eq. (2.2), is pair decomposable. Hence we can always write

$$A_{J0}(\mathbf{R}) = \sum_j a_{J0}(\mathbf{r}_{j0}), \tag{3.8}$$

with $\mathbf{r}_{j0} = \mathbf{r}_j - \mathbf{r}_0$ the vector from the solute center of mass to the jth solvent. But, consistent with the vibrational relaxation discussion,[53] we expect that for a given liquid configuration $\mathbf{R}$, the markedly short range of the $a_{J0}(r)$ functions will guarantee that this sum will be dominated by a single, nearest-neighbor solvent $j(\mathrm{nn})$.

$$A_{J0}(\mathbf{R}) \approx a_{J0}(\mathbf{r}_{j(\mathrm{nn})0}). \tag{3.9}$$

Moreover, whenever that near neighbor is closer to the solute than it is to any other molecule in the system [i.e., whenever this solvent molecule is a *mutual* nearest neighbor (mnn)], we expect that the dynamics of this pair will be governed just by the intrapair forces. The equation of motion is then simply

$$\mu \ddot{r}_{j(\mathrm{mnn})0} = -u'(r_{j(\mathrm{mnn})0}), \tag{3.10}$$

with μ the solute-solvent reduced mass, $u(r)$ the isotropic part of the solute–solvent pair potential, and $u'(r) = du/dr$. Pursuing this reasoning to its logical conclusion, one also expects liquid configurations with mnn solute–solvent pairs to dominate the configurational average in Eq. (3.7). Configurations with solvents that are near neighbors but *not* mutual near neighbors should have noticeably smaller couplings (inasmuch as their solute–solvent distances are necessarily larger). We should therefore take $j(\mathrm{nn}) = j(\mathrm{mnn})$ in Eq. (3.9) as well.[53,55]

Differentiating Eq. (3.9) and substituting the result in Eq. (3.7) then, gives our instantaneous-pair theory for the high-frequency rotational friction

$$-\ddot{\eta}_J(t) = (b_J/2k_BT)\langle (da_{J0}/dr)_{r(t)} \times (da_{J0}/dr)_{r(0)} \dot{r}(t)\dot{r}(0)\rangle_{r=r_{j(\mathrm{mnn})0}}, \tag{3.11}$$

where the average is over the initial values and velocities of the mutual-nearest-neighbor solute–solvent distances and the dynamics is governed simply by Eq. (3.10). The omission of all of the many-body features of the dynamics obviously renders this formula incapable of including any of the collective aspects of rotational relaxation. Yet, because it includes the dependence of the anisotropy coefficients $a_{J0}(r)$ on r, this formula does take into account the important nonlinearities in the solute–solvent coupling. Its use of the full two-body force means, similarly, that it manages to encompass critical portions of the dynamical anharmonicity.[53]

To recover the connection with the liquid's instantaneous normal modes, we now take this approximation back a step. Suppose we continue to insist that the coupling nonlinearities are crucial, but we remove all traces of the dynamical anharmonicities. In particular, instead of employing the exact anharmonic dynamics of the solute–solvent pair, we can treat the pair's dynamics as that of a single harmonic, instantaneous normal mode—a *binary mode*[36,56] of frequency ω_0 subject to an instantaneous force f_0, both quantities being determined by derivatives of the pair potential $u(r)$ at the instantaneous configuration $r_{j(\mathrm{mnn})0}(0)$.

$$\mu\omega_0^2 = u''[r_{j(\mathrm{mnn})0}], \quad f_0 = -u'[r_{j(\mathrm{mnn})0}]. \tag{3.12}$$

Since the solute–solvent pair now obeys the standard INM dynamics

$$r_{j(\mathrm{mnn})0}(t) = r_{j(\mathrm{mnn})0}(0) + (f_0/\mu\omega_0^2)(1-\cos\omega_0 t) + (v_0/\omega_0)\sin\omega_0 t, \tag{3.13}$$

with initial velocity v_0, but the friction is still given by Eq. (3.11), what we end up with is a fully *nonlinear INM theory* based on this same instantaneous pair perspective.[53]

In the pair language, the analogue of our previous, linear, theory would come by regarding the derivatives da_{J0}/dr in Eq. (3.11) as constants, a requirement equivalent to Eq. (3.4). By going beyond this linearity while not allowing for the full anharmonicity of the dynamics, we can test the extent to which harmonic modes remain a useful concept when we stray beyond the safe haven of the INM band.

IV. H_2 AND D_2 IN LIQUID Ar: MODEL AND CALCULATIONAL DETAILS

A. The model

As we indicated in Sec. I, the large rotational constants and nearly spherical shape of H_2 and its isotopomers make them natural candidates for studying the dynamics of discrete rotational states in liquids. Though much of the previous experimental and theoretical work to date has focused on these molecules dissolved in H_2O,[10–12,14] in order to make sure that we understand the fundamentals, we deliberately limit ourselves here to the more straighforward situation of H_2 and D_2 in $Ar_{(l)}$.[13]

As with the study of Xiao and Coker,[13] we shall take the Ar–Ar interaction to be of the Lennard–Jones form

$$u_{vv}(r) = 4\epsilon[(\sigma/r)^{12} - (\sigma/r)^6],$$

with the standard parameters,[57] $\sigma = 3.405$ Å and $\epsilon/k_B = 119.8$ K, and we shall consider just the single room temperature (high-density supercritical) thermodynamic state with temperature T and density ρ given by

$$k_BT/\epsilon = 2.5, \quad \rho\sigma^3 = 0.95.$$

The H_2–Ar part of the interaction is well described by the Leroy–Hutson potential,[58] the result of a careful fit to spectroscopic, scattering, and thermodynamic data. The particular version we use here has the bond length fixed at 0.77

TABLE I. Rotational friction spectra for H_2 and D_2 dissolved in dense supercritical argon.[a]

Solute	k	B_k (10^{-22} J)	E_k (cm^{-1})	G_k (cm^{-1})	Rel. dev.[b]
H_2	1	2.12	341.9	257.5	0.11
	2	0.366	160.9	71.6	
	3	0.677	44.3	65.4	
D_2	1	0.780	298.3	134.9	0.10
	2	0.173	177.3	7.34	
	3	1.69	166.8	231.8	

[a]Parameters for the fits of each friction spectrum $\rho_2(\omega)$ to ω times a sum of three Gaussians ($k=1,2,3$), with B_k, E_k, and G_k, respectively, the amplitude, mean, and width of each Gaussian.
[b]Relative deviation of the fitted spectrum from the simulated spectrum: $\int d\omega|\rho_{\rm fit}(\omega)-\rho_{\rm data}(\omega)|/\int d\omega\rho_{\rm data}(\omega)$.

Å. Specifically, the pair potential between the solute with center of mass at $\mathbf{r}_0$ and the jth Ar solvent atom (located at $\mathbf{r}_j$) is written in the form

$$u_{uv}(r_{0j},\Theta_j)=u_0(r_{0j})+u_2(r_{0j})P_2(\cos\Theta_j), \tag{4.1}$$

where $r_{0j}=|\mathbf{r}_0-\mathbf{r}_j|$ and Θ_j is the angle between $\hat{\Omega}_0$, the bond axis of the solute, and $\mathbf{r}_{0j}$. This form lends itself rather easily to a spherical harmonic decomposition of the type assumed in Eq. (2.2). Since

$$P_2(\cos\Theta_j)=(4\pi/5)\sum_{M=-2}^{2} Y_{2M}^*(\mathbf{r}_{0j})Y_{2M}(\hat{\Omega}_0),$$

the total anisotropic solute–solvent interaction can be written

$$V(\Omega_0,\mathbf{R})=\sum_j u_2(r_{0j})P_2(\cos\Theta_j)$$

$$=\sum_{M=-2}^{2} A_{2M}(\mathbf{R})Y_{2M}(\Omega_0),$$

leaving us with a single nonvanishing relevant anisotropy coefficient, that for $J=2$.

$$A_{20}(\mathbf{R})=(4\pi/5)\sum_j u_2(r_{0j})Y_{20}(\mathbf{r}_{0j}). \tag{4.2}$$

Because the only J that contributes in this model is $J=2$, we shall be able to omit the sum over J (and the J index) in all of our subsequent equations.

To evaluate the friction within our weak anisotropy assumption then, we need only to evaluate the time correlation function $C(t)=\langle A_{20}(t)A_{20}(0)\rangle$ with the initial conditions and the dynamics governed by the isotropic part of the interaction

$$V_B(\mathbf{R})=\sum_j u_0(r_{0j})+\sum_{\substack{j,k\\(j<k)}} u_{vv}(r_{jk}), \tag{4.3}$$

that is, with the solute regarded as a sphere. In fact, even this expression can be simplified. We note, as did Xiao and Coker,[13] that the elaborate $u_0(r)$ function of LeRoy and Hutson[58] is well approximated in practice as a Lennard–Jones potential with $\sigma=3.1375$ Å and $\epsilon/k_B=59.145$ K.

All of the calculations performed with D_2 were carried out using precisely the same $u_0(r)$ and $u_2(r)$ potentials as those used with H_2.

B. Simulation, INM, and instantaneous-pair-theory calculations

Molecular dynamics simulations were carried out on a sample consisting of the solute and 107 Ar atoms with the trajectories propagated via the velocity Verlet algorithm using 2.16 fs time steps.[59] A trajectory consisting of 1.05×10^7 time steps was employed to obtain torque correlation functions. When ordinary (linear) INM analysis was required, 40 000 liquid configurations were selected by sampling every 108 fs along a trajectory and diagonalizing the dynamical matrix each time.[60] The resulting eigenvalues and eigenvectors were used to construct the frequencies ω_α^2 and coupling coefficients

$$c_\alpha=(15/4\pi)^{1/2}\partial A_{20}/\partial q_\alpha,$$

for each configuration and each mode α. Inasmuch as the friction spectrum, Eq. (3.6), is quite noisy in the high-frequency region, when we needed to take Fourier transforms we found it useful to fit the real-frequency part of the spectrum first to the form[61]

$$\rho(\omega)=\omega\sum_{k=1}^{3} B_k\exp\{-[(\omega-E_k)/G_k]^2\}.$$

The parameters for the fits are given in Table I. The imaginary portion of the spectrum ($\omega_\alpha^2<0$) turns out to be rather small and, in any case, is irrelevant to energy relaxation at the level of theory pursued in this article.

Instantaneous pair theory calculations require only that we be able to evaluate one-dimensional correlation functions involving the solute and its nearest neighbor. The averaging over initial conditions for these correlation functions, Eq. (3.11), was accomplished by first computing the radial distribution function for the mutual-nearest-neighbor distances (based on a sample of 10^6 independent configurations from the molecular dynamics simulation), and then performing the two-dimensional integral over distance and the velocity using Simpson's rule. The dynamics for the fully anharmonic version of instantaneous-pair theory was evaluated by solving the one-dimensional pair equation of motion, Eq. (3.10), using the velocity-Verlet algorithm with the same time step as in the many-body simulation.

TABLE II. Validity of perturbation theory for H_2 dissolved in dense supercritical argon.

(l,l')[a]	(2,0)	(3,1)	(4,2)	(5,3)	(6,4)	(7,5)	(8,6)
$(V_{ll'}/\Delta E_{ll'})$[b]	0.049	0.019	0.011	0.0076	0.0056	0.0044	0.0035

[a]Total angular momentum quantum numbers for each pair of rotational energy levels considered. Only pairs with $\Delta l = \pm 2$ are connected by nonzero matrix elements of the Hamiltonian.
[b]Ratio of $V_{ll'}$, the root-mean-square average of the matrix element coupling each pair, to $\Delta E_{ll'} = E_l - E_{l'}$, the gap between the isolated-molecule energy levels of the pair.

V. H_2 AND D_2 IN LIQUID Ar: RESULTS

A. Exact and weak-coupling relaxation rates

The first issue for us to confront is the level of accuracy we can expect from our weak coupling theory. The entire development in the article relies on our somewhat counterintuitive claim that the dynamics of a liquid surrounding a spherical solute is all that is necessary to understand the rotation of a diatomic in a liquid (or at least is all that is required for the limited class of systems considered here). So just how reliable is this assumption?

The criterion we put forth for the validity of the quantum perturbation theory, Eq. (2.5), is something we can check directly for any pair of rotational energy levels l and l' that our solvent might induce a transition between [which, according to Eq. (2.22), are those for which $|\Delta l| = 2$]. Following the dictates of Eq. (2.5), we compare, in Table II, the matrix elements coupling various pairs of levels with the gas-phase energy level spacing between the levels. Since the matrix elements are identical for H_2 and D_2 (because they depend only on the solute-solvent potential) while the energy spacings differ by a factor of 2 (because of the differing moments of inertia), the coupling-to-energy-gap ratios are twice as large for D_2 as they are for H_2. However even with D_2, the ratio is well within the realm one would expect for a valid perturbative treatment. Evidently hydrogen in Ar can be thought of as a prototypical weak-torque situation in the sense of Eq. (2.26).

The second key step in our theory, though, was to write down a weak-coupling version of the classical friction. It is not out of the question that our perturbation criterion could be satisfied without the anisotropy coefficients being as uncorrelated with the solute orientation as we assumed, but here again, we can perform a direct test. In Fig. 1 we plot the exact rotational friction obtained by simulating the torque autocorrelation function, Eq. (1.4b), and compare the results with the weak-coupling friction, Eq. (2.19) with Eqs. (2.15) and (4.2). Note that the exact friction uses the full LeRoy–Hutson potential[58] in order to evaluate the time evolution of the torque, whereas the weak-coupling version calculates the dynamics from just the isotropic portion of this potential, the $u_0(r)$ in Eq. (4.1). Despite these differences, the two versions are obviously barely distinguishable on the scale of the graphs, both for H_2 and D_2. Repeating the weak-coupling calculation with the Xiao–Coker Lennard–Jones version of $u_0(r)$ (not shown) yields results almost identical to those from the LeRoy–Hutson weak-coupling treatment. We shall

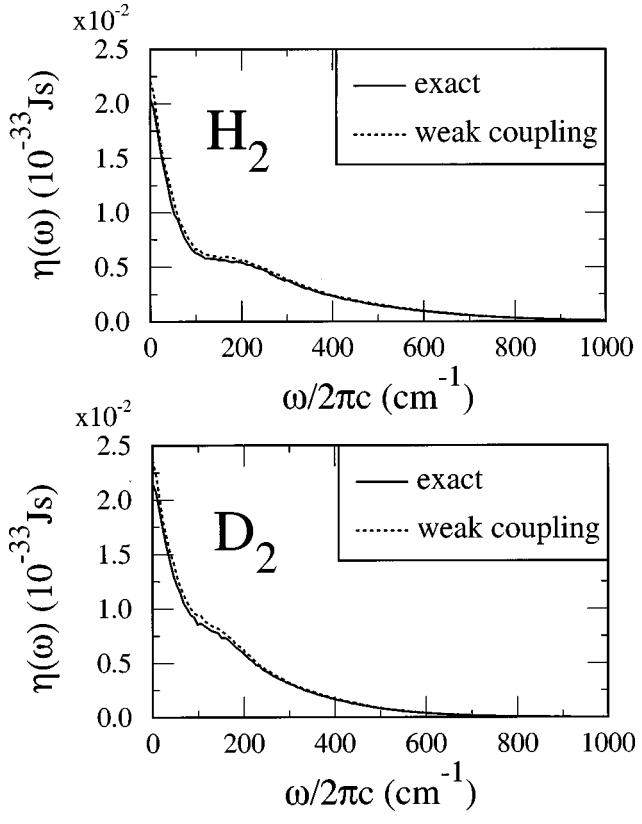

FIG. 1. The rotational friction felt by H_2 (top panel) and D_2 (bottom panel) dissolved in dense supercritical Ar. Each panel compares the exact friction (defined in terms of the classical torque autocorrelation function) with the weak-coupling friction (derived from the classical anisotropy autocorrelation functions). Both correlation functions are evaluated by molecular dynamics, but for the former the dynamics is based on the full LeRoy–Hutson potential for the solute–solvent interaction, whereas for the latter only the isotropic part of the LeRoy–Hutson potential is used.

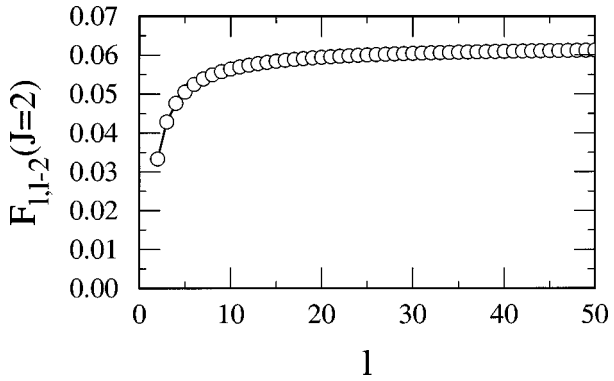

FIG. 2. The angular-momentum-coupling coefficients $F_{l,l-2}(2)$ as a function of l. Through leading order in the anisotropy of the solute–solvent potential, these F's are the coefficients governing the $l \to l-2$ rotational transitions induced in a homonuclear diatomic solute.

TABLE III. Rotational population relaxation rates for H_2 dissolved in dense supercritical argon.[a]

$l' \to l$	$\Omega/2\pi c$[b] (cm^{-1})	MD[c]	Linear INM[c]	IP[d]	Nonlinear INM[d]	$k_{l\to l'}/k_{l'\to l}$
2→0	341	0.28	0.43	0.19	0.27	0.97
3→1	569	0.14	0.17	0.12	0.12	0.15
4→2	796	5.3×10^{-2}	1.4×10^{-2}	5.0×10^{-2}	3.8×10^{-2}	3.9×10^{-2}
5→3	1024	1.7×10^{-2}	2.3×10^{-4}	1.8×10^{-2}	1.6×10^{-2}	1.1×10^{-2}
6→4	1251	4.8×10^{-3}	8.4×10^{-7}	6.1×10^{-3}	6.1×10^{-3}	3.5×10^{-3}
7→5	1479	1.4×10^{-3}	6.6×10^{-10}	1.9×10^{-3}	2.0×10^{-3}	1.1×10^{-3}
8→6	1706	4.0×10^{-4}	1.1×10^{-13}	5.9×10^{-4}	6.9×10^{-4}	3.6×10^{-4}
9→7	1934	1.4×10^{-4}	3.8×10^{-18}	1.8×10^{-4}	2.5×10^{-4}	1.2×10^{-4}
10→8	2161	6.8×10^{-5}	2.9×10^{-23}	5.2×10^{-5}	1.1×10^{-4}	3.8×10^{-5}

[a]Transition rates $k_{l\to l'}$ for the downward transitions from energy level l to energy level l', reported in ps^{-1}. The corresponding rates for the upward transitions are prescribed by the detailed-balance ratios given in the last column.
[b]Transition frequencies $\Omega \equiv (E_l - E_{l'})/\hbar$ with the E_l the isolated-molecule energy levels.
[c]Evaluation of the perturbation theory result by exact molecular dynamics simulation (MD) and by linear INM theory.
[d]Evaluation of the perturbation theory result by pair theories: ''IP'' denotes the full instantaneous-pair theory and ''nonlinear INM'' refers to the IP approach with the pair dynamics treated by INM theory.

therefore be able to make use of the computationally simpler Xiao–Coker potential for all of our subsequent calculations.

Given that our basic result for the relaxation rate, Eq. (2.20), seems to be sensible, it is natural to ask which of factors in this expression actually end up controlling the rate. Focusing specifically on H_2 and D_2 in Ar [and therefore on Eq. (2.23)], it is clear that the detailed-balance prefactor,

$$[1+e^{-\hbar\Omega\beta}]^{-1},$$

is going to be a rather slowly varying function of the transition frequency $\Omega_{ll'}$ under ambient conditions. The angular momentum coupling coefficients $F_{ll'}(2)$ will be important in limiting the allowed transitions to those for which $l' = l \pm 2$, [Eq. (2.22)]. However for the transitions which are allowed, explicit calculation tells us that $F_{ll'}(2)$ will be a similarly slowly varying function of the transition frequency (Fig. 2). A glimpse at this figure, or equivalently, at the expression derived from the analytical formula for the 3-j symbol,[62]

$$F_{l,l-2}(2) = [l(l-1)/4(2l+1)(2l-1)],$$

shows that F goes smoothly from its lowest possible value of 1/30 (for the 2→0 transition) to 1/16 (as $l\to\infty$).

What must be the principal determinant of the rotational energy relaxation rate then, is the rotational friction itself. As one can see from the tabulated level-to-level transition rates for H_2 (Table III) and D_2 (Table IV), the rates drop by several orders of magnitude as one progresses through the first nine allowed transitions—precisely as we would have expected from the behavior of the friction portrayed in Fig. 1. We turn therefore, to considering the molecular origins of this friction.

B. Linear INM analysis

Within linear INM theory, Eqs. (3.5) and (3.6), the frequency dependence of the rotational friction arises mainly from the shape of the corresponding rotational influence spectrum, Fig. 3.[31,63] As is now familiar from our studies of solvation and vibrational relaxation,[35–37,52] as well as from

TABLE IV. Rotational population relaxation rates for D_2 dissolved in dense supercritical argon.[a]

$l' \to l$	$\Omega/2\pi c$[b] (cm^{-1})	MD[c]	Linear INM[c]	IP[d]	Nonlinear INM[d]	$k_{l\to l'}/k_{l'\to l}$
2→0	171	0.51	0.70	0.29	0.25	2.2
3→1	285	0.38	0.62	0.28	0.39	0.59
4→2	398	0.23	0.28	0.18	0.19	0.27
5→3	512	0.12	5.5×10^{-2}	0.10	7.9×10^{-2}	0.13
6→4	626	5.4×10^{-2}	7.0×10^{-3}	5.4×10^{-2}	4.3×10^{-2}	7.1×10^{-2}
7→5	740	2.3×10^{-2}	6.6×10^{-4}	2.7×10^{-2}	2.4×10^{-2}	3.9×10^{-2}
8→6	854	9.8×10^{-3}	4.1×10^{-5}	1.2×10^{-2}	1.2×10^{-2}	2.2×10^{-2}
9→7	968	4.1×10^{-3}	1.6×10^{-6}	5.7×10^{-3}	5.9×10^{-3}	1.2×10^{-2}
10→8	1081	1.7×10^{-3}	3.8×10^{-8}	2.6×10^{-3}	2.7×10^{-3}	6.8×10^{-3}

[a]Transition rates $k_{l\to l'}$ for the downward transitions from energy level l to energy level l', reported in ps^{-1}. The corresponding rates for the upward transitions are prescribed by the detailed-balance ratios given in the last column.
[b]Transition frequencies $\Omega \equiv (E_l - E_{l'})/\hbar$ with the E_l the isolated-molecule energy levels.
[c]Evaluation of the perturbation theory result by exact molecular dynamics simulation (MD) and by linear INM theory.
[d]Evaluation of the perturbation theory result by pair theories: ''IP'' denotes the full instantaneous-pair theory and ''nonlinear INM'' refers to the IP approach with the pair dynamics treated by INM theory.

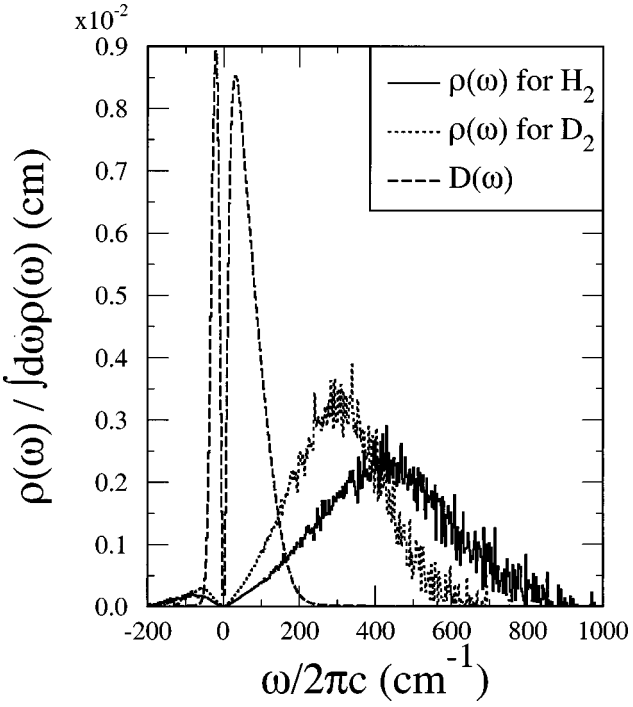

FIG. 3. Normalized rotational friction spectra $\rho(\omega)=\rho_2(\omega)$ for H_2 and D_2 dissolved in dense supercritical Ar. Shown for comparison is the instantaneous-normal-mode density of states for the solution, $D(\omega)$, also normalized to unit area. As is conventional, imaginary frequencies are plotted as negative frequencies. In this and all of the succeeding figures, the solute–solvent interaction is modeled with the isotropic Xiao–Coker potential.

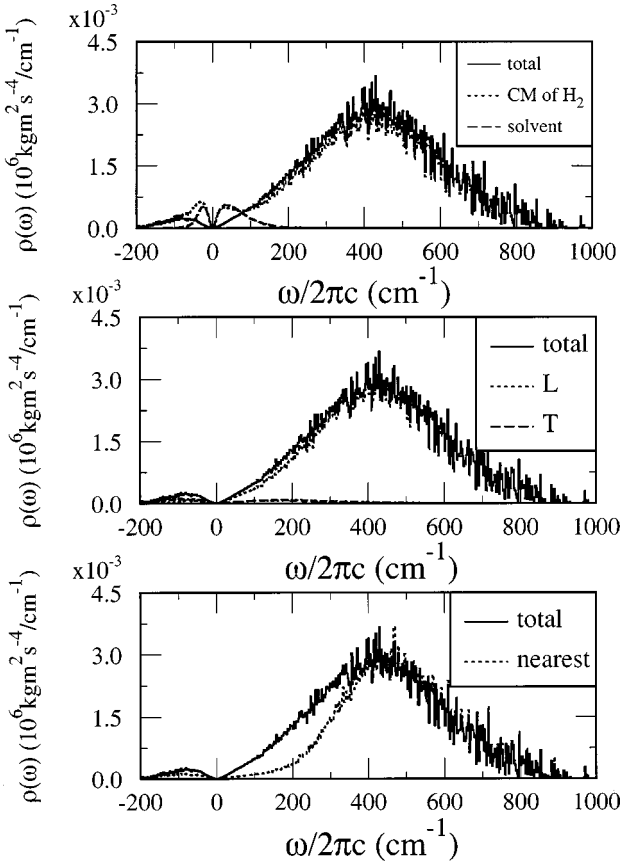

FIG. 4. Various projections of the rotational friction spectrum for H_2 dissolved in dense supercritical argon. *Top panel*: partitioning between the center-of-mass translation of the H_2 solute (CM) and the motion of Ar atoms (solvent). *Middle panel*: partitioning between longitudinal (L) and transverse (T) solvent dynamics (i.e., motion parallel and perpendicular to the solute-center-of-mass/solvent vector, repectively). *Bottom panel*: comparison between the component arising from the nearest-neighbor solvent (nearest) and the total friction spectrum (total).

our previous work on (classical) rotational relaxation,[31] influence spectra invariably emphasize higher values of ω^2 than the solvent's density of states (DOS) does. In particular, the $(\omega^2<0)$ imaginary frequencies, which comprise a significant fraction of the DOS, make only a miniscule contribution to the influence spectrum (and no contribution whatsoever to the level-to-level transition rates—which involve the friction only at certain discrete real frequencies).

There is, however, an interesting difference between the present influence spectra and others we have studied. In all of the previous work, the emphasis on higher frequencies took the form of a shift in the frequency of the *maximum* solvent response with little, if any, change in the overall spectral range of that response. This kind of behavior is a natural consequence of the fact that it is the INM bands that define the natural frequency range of intermolecular motion in our solvents. Figure 3, though, seems to have the majority of its friction spectral density lying outside the INM band. So, where does this new high-frequency response come from?

The answer becomes apparent if we project out of the influence spectra the portion arising from the center-of-mass motion of the solute (Fig. 4). It is clearly the net translation of our very light solutes that generates the bulk of the high-frequency response predicted by linear INM theory.[64] A calculation of the areas under the projected spectra reveals that center-of-mass translation actually generates on the order of 90% of the entire response (Table V). Interestingly, since our bath does include the motion of the solute center of mass along with the motion of all of the solvent atoms, this same high frequency dynamics must be present in the original density of states. But since it corresponds to just a few degrees of freedom, it is invisible against the background created by the macroscopic number of solvent degrees of freedom. In the influence spectrum, by contrast, the background comes

TABLE V. Mechanism of rotational relaxation for H_2 and D_2 dissolved in dense supercritical argon.[a]

Solute	Solute center of mass[b]	Longitudinal[c]	Nearest solvent[d]
H_2	94.4	92.2	82.8
D_2	89.2	92.5	82.3

[a]Percentage contributions of the indicated dynamical processes to the total rotational friction spectrum.
[b]Partitioning between motion of the solute-center-of-mass and solvent translational motion.
[c]Partitioning between solvent motion parallel (longitudinal) and perpendicular (transverse) to the instantaneous solvent/solute-center-of-mass vector.
[d]Partitioning between solvent contributions arising from the solvent atom instantaneously nearest the solute center of mass and all of the remaining solvent atoms.

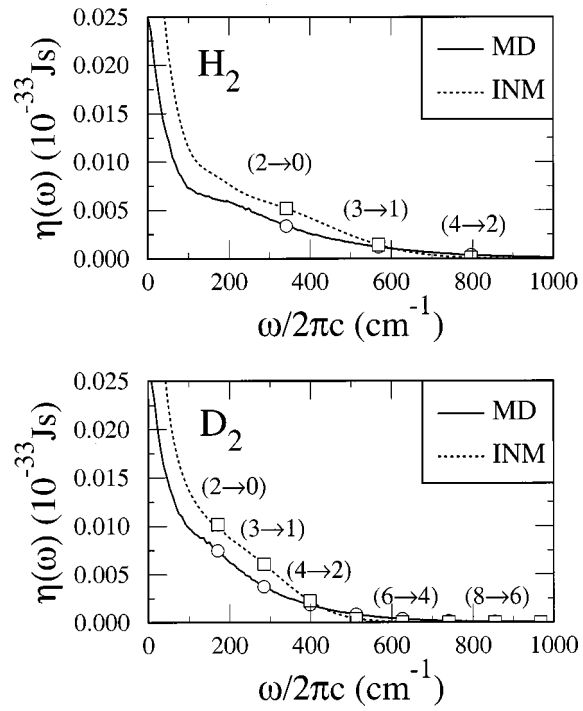

FIG. 5. Comparison of linear instantaneous-normal-mode (INM) predictions for rotational friction with exact molecular dynamics results (MD) for both H_2 and D_2 dissolved in dense supercritical Ar. The open symbols mark the transition frequency for each allowed $l \rightarrow l-2$ rotational transition (the identity of which is indicated directly above the symbol).

solely from those few solvents close enough to the solute to be able to create a significant torque.

We can refine our ideas about the mechanism of rotational energy relaxation still more by imagining sitting in the solute's own reference frame and watching the solvent atoms move with respect to the solute. From this perspective we know that what we still need to specify in order to define the mechanism is the geometry and number of *solvent* atoms most critically involved in the dynamics. We can collect this information as well via suitable projections of the influence spectrum (Fig. 4 and Table V).[32] The results now look strikingly similar to our previous findings for solvation and for vibrational and rotational relaxation with much heavier solutes:[32,33,36,37,52] More than 90% of the influence spectrum stems from longitudinal solvent motion—from motion parallel to the instantaneous solute-center-of-mass/solvent vector—and nearly 83% of the spectrum arises from the single solvent atom in each configuration that is nearest the solute center-of-mass. In the language of the original laboratory frame, then, we would say that the key event in the relaxation process almost always consists of the solute moving directly towards a single key solvent atom.

The linear INM theory should not only be useful for assigning the mechanism, it should be reasonably accurate in predicting the rotational friction[31] and thus the actual rotational energy relaxation rates. Indeed, as one can see from Fig. 5 and from Tables III and IV, the predicted values of the rotational friction track those of the exact molecular dynamics quite adequately for the first few allowed rotational transitions. As long as we are considering transition frequencies Ω within the INM band (being careful to include the solute–translation portion of the band), INM theory seems to nicely capture—and explain—the falloff of the relaxation rates with increasing rotational quantum number.

C. Instantaneous-pair and nonlinear INM analysis

Further inspection of Tables III and IV makes quite clear that linear INM theory does *not* suffice once one enters or goes beyond the upper edge of the INM band. For H_2, the predicted rates for transitions with frequencies larger than or of the order of 800 cm^{-1} are far too small, as are the D_2 rates for frequencies above 500 cm^{-1}. These results are, of course, precisely in line with our comments in Sec. III B: once the density of INM modes at the relevant frequency becomes too low, the one-quantum-of-solute-to-one-quantum-of-solvent resonant energy transfer mechanism embodied in linear INM theory no longer provides the fastest route to relaxation.[53]

The mechanistic information we gathered from our linear INM investigations, however, continues to be worth listening to even when we are well beyond the INM band edge. The strong reliance we found on the one-dimensional motion of a key solvent partner suggests that the instantaneous-pair theory discussed in Sec. III B might very well be worth trying. While we know that a pair theory cannot capture any of the collective character of the relaxation, it is possible that the ability to incorporate both anharmonic dynamics and nonlinear coupling might more than make up for this deficiency at these high frequencies. The results for H_2, shown in Table III and in Fig. 6, bear out these expectations. The instantaneous-pair theory predicts rates in excellent agreement with molecular dynamics—and consistently better than those of linear INM theory. In fact, the pair theory agrees quantitatively with molecular dynamics results spanning some three decades in relaxation rates, Fig. 7.

This numerical superiority to linear INM theory is actually revealing. For frequencies well inside the INM band (less than 200 cm^{-1}), the linear INM predictions for the friction are significantly better than the pair theory (Fig. 6), just as we found in our previous studies of vibrational relaxation.[53] Indeed, inside the band, the instantaneous-pair rates fall well below the exact results since a pair theory lacks the ability to represent collective dynamics. However, the only frequencies relevant to the rotational transitions of H_2 fall outside the band of the neat solvent, so these collective dynamics are never needed. Supporting evidence for these ideas is also found in the relaxation rates of D_2, Table IV and Fig. 7. The instantaneous-pair-theory continues to agree nicely with molecular dynamics outside the liquid band. With the lower rotational transition frequencies of D_2, though, the first few transitions now fall inside the band—and as we would have expected, are somewhat better described by linear INM theory than by instantaneous-pair theory.

We could, of course, be content with this agreement, but it is telling to consider what would happen to these pair results if we no longer insisted on an anharmonic treatment of the dynamics. That is, suppose we were to adopt the nonlinear INM theory put forth in Sec. III B: we allow the pair torque whose evolution we are studying to depend on the

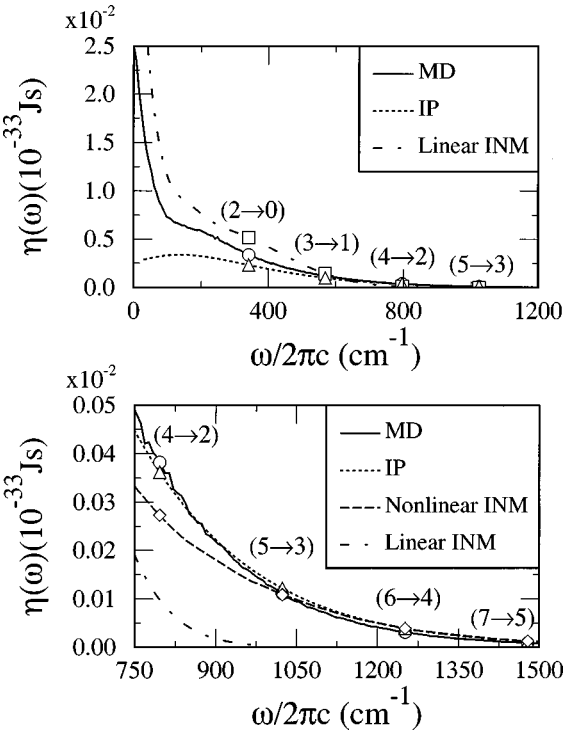

FIG. 6. Pair-theory predictions for the rotational friction of H_2 dissolved in dense supercritical Ar. Both panels compare the instantaneous-pair theory predictions (IP) with molecular dynamics (MD) and linear INM predictions. The bottom panel examines the high-frequency response in more detail and compares all three predictions with the results from a nonlinear INM rendition of the pair theory. Note the fifty-fold magnification of the vertical scale in the bottom panel. As in Fig. 5, the open symbols mark the transition frequencies for the indicated $l \rightarrow l-2$ rotational transitions.

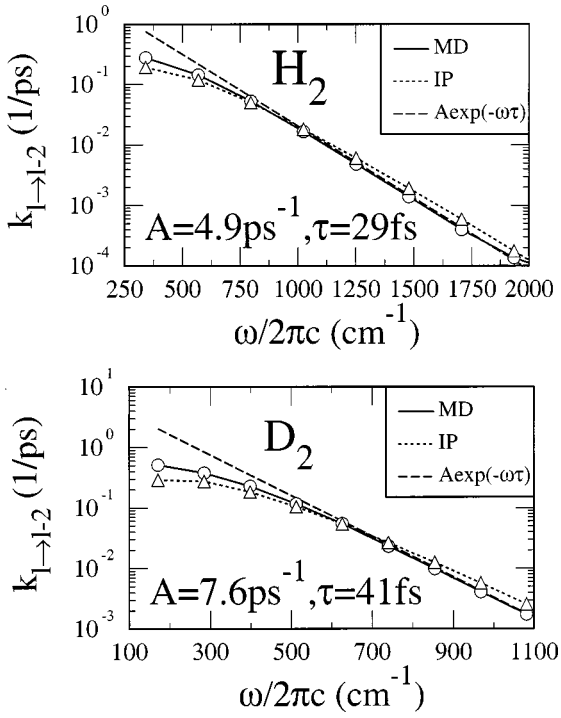

FIG. 7. Exponential-gap-law behavior for rotational energy relaxation rates of H_2 and D_2 dissolved in dense supercritical Ar. The molecular dynamics (MD) and instantaneous-pair (IP) predictions for the rate constants of the $\Delta l = -2$ rotational transitions are shown as a function of transition frequencies and compared with the empirical exponential-gap-law predictions (long-dashed lines) obtained by fitting to the MD results. Open symbols mark the transition frequencies for each allowed transition.

pair separation in its exact, fully nonlinear, fashion, but we now regard the pair dynamics as being controlled by a single INM harmonic mode. Physically, this approach is hardly unreasonable. It basically postulates a multiphonon scenario in which the nonlinear solute–solvent coupling generates overtones of the solvent INM modes and these harmonics then account for the high-frequency relaxation.[53,54,65] Nonetheless, one could wonder about the internal consistency of such an approach. In effect it says that the same anharmonicity that is unimportant for the underlying solute–solvent dynamics is vital for the solute–solvent coupling being driven by that dynamics. So can it, in fact, lead to a sensible picture of rotational relaxation?

From the outcome of this kind of nonlinear INM treatment presented in Tables III and IV and displayed in the bottom panel of Fig 6, it is clear that we do not need to include the dynamical anharmonicity in order to understand rotational friction. Nonlinear INM calculations produce transition rates in excellent agreement with both the full instantaneous-pair theory and the exact many-body molecular dynamics in the high-frequency regime. In fact, taken together with the linear INM theory for relaxation occurring within the INM band, it is evidently possible to give a harmonic-mode interpretation for the complete range of rotational transitions. There clearly are a variety of different places that anharmonicity can enter this problem—and, interestingly, they all seem to be surprisingly well insulated from one another.[53]

As a final comment, we should note that all of these calculations end up leading to fundamentally the same kind of result, that rotational energy relaxation rates in liquids obey the same kind of exponential-gap-law they tend to in the gas phase.[66] That is, for all but the lowest transitions, Fig. 7 tells us that it is fairly accurate to write

$$k_{l \rightarrow l'} = k_0 \exp(-|\Omega_{ll'}|\tau), \tag{5.1}$$

with k_0 and τ constants. The frequency dependence of our basic expression for the transition rate, Eq. (2.23), might seem unlikely to yield such a dependence on the transition frequency Ω, but as we noted earlier, both the detailed-balance factor and the F angular-momentum coupling factor are nearly constant at high frequencies, leaving the bulk of the frequency dependence in the friction. As with our previous examination of vibrational friction,[53] we indeed do find empirically that the asymptotic form of our friction is exponential

$$\hat{\eta}(\omega) = \eta_0 \exp(-\omega\tau).$$

Amusingly, the values of τ that leads to the best fits to our molecular-dynamics-derived friction are on the order of the characteristic nonlinear time scales t_0 found from our previous instantaneous-exponential formulation of nonlinear INM theory[53]

$$t_0 = (2\mu/\alpha_0^2 k_B T)^{1/2},$$

$$\alpha_0 = \mu\omega_0^2/f_0 = -(d\ln u'(r)/dr)_{r(0)},$$

where the instantaneous frequency ω_0 and instantaneous force f_0 are defined by Eq. (3.12). Average values of t_0 were found to be 21 and 29 fs for H_2 and D_2, respectively, in reasonable accord with the τ values of 29 and 41 fs we found from our fits to the molecular dynamics results.[67]

VI. CONCLUDING REMARKS

It would not have been unreasonable to presume that how a liquid extracts a solute's vibrational energy would have little to do with how it removes rotational energy. The degrees of freedom themselves just seem to be fundamentally disparate. From a classical perspective, vibrational energy is constantly interconverting between kinetic and potential energy while the rotational energy of a free rotor is always kinetic. Quantum mechanically, the low-lying energy levels for most vibrations are nearly equally spaced, meaning that vibrations tend to have a single fundamental frequency, whereas rotational energy level spacing increases monotonically for linear molecules. Worse still, the kinematics and symmetries of the two kinds of motion are about as different as one could imagine. It is easy to imagine that solvents might very well need to interact with the two degrees of freedom quite differently.

What this article has shown, though, is that molecular rotations with well-defined energy levels seem to relax in ways remarkably close to those of vibrations. Most notably, rotational energy relaxation obeys a *rotational Landau–Teller relation* in precise analogy to the relation obeyed by vibrations: the rate of level-to-level relaxation is proportional to the frequency-dependent friction exerted by the solvent evaluated at the frequency of the transition. That rotational energy relaxation obeys some sort of fluctuation-dissipation theorem is hardly a surprise; what may not have been quite so obvious is that the solvent fluctuations that turn out to govern the dissipation of rotational energy have such a close analogy to the ones controlling vibrational energy. Both, in particular, are controlled by precisely the same friction that governs the regression of their respective velocities. Admittedly, the rotational friction spectral densities we computed in this article have a spectral range well beyond what we are used to seeing for vibrational relaxation in aprotic solvents.[36,37,68] The differences, though, come from the unusually low molecular weight of our solutes. When we compute the vibrational friction spectral density for H_2 we find a result virtually identical to that for the rotational friction.[69] Both frictions are dominated instantaneously by the same few-body dynamics, so the solvent presents largely the same spectral density to both vibrational and rotational motion.[36,37]

The fact that we were able to convert the problem of rotational energy level lifetimes into a study of classical rotational friction is what really gave us this insight into the origins of the spectral density. With this relationship we found that we could use molecular dynamics simulations to obtain exact answers (exact, at least, within the basic weak-coupling framework of this article). More than that, though, the relationship allowed us to use instantaneous-normal-mode analysis of the friction to propose an interpretation of the underlying molecular mechanisms. Projection of the INM influence spectrum reveals the essentially few-body character of the instantaneous relaxation mechanism, with the key step the longitudinal motion of the H_2 (or D_2) center of mass relative to a single near-neighbor solvent atom. The INM treatment of the solution automatically suggests, moreover, that there really is a band of collective motions spanning the liquid's own natural time scales. Indeed, our linearized INM theory takes this idea sufficiently literally that it interprets a Landau–Teller law as prescribing a 1:1 energy transfer between the solute and these liquid modes, leading to a prediction that relaxation rates should decay rapidly for transition frequencies outside the band.

Both the basic predictions for the rotational friction and the precipitous fall-off of relaxation rates are confirmed reasonably well by molecular dynamics. The mechanistic ideas are actually confirmed in even greater detail by the success of the instantaneous-pair model for the rotational energy relaxation rates. Relaxation rates for all but the lowest few rotational transitions obey an exponential gap law, a law reproduced strikingly well by the one-dimensional pair dynamics predicted from the isotropic part of the solute/mutual-nearest-neighbor-solvent interaction. The agreement with molecular dynamics could probably be improved a bit by employing the full anisotropic interaction (as we did in our previous vibrational studies),[53] but the critical molecular details are clear. We can even interpret this outside-of-the-band behavior as a multiphonon extension of instantaneous-normal-mode ideas. The high-frequency results are well reproduced by regarding the pair dynamics as a single harmonic mode, provided we allow for the fully nonlinear way in which the dynamics of the torque depends on the mode. This nonlinearity is evidently sufficient to generate the high-frequency overtones necessary for resonant energy transfer.

It is probably worth emphasizing that all we have done in this article is to look at rotational-energy-level-to-rotational-energy-level transition rates. While our findings certainly bear on a variety of spectroscopic studies of hydrides in solution, none of these results correspond to direct experimental measurements. We would therefore like to close with a few comments on possible connections with experiment. Perhaps the conceptually simplest experiment pertinent to our calculations (albeit the most difficult to carry out) would be a pump-probe measurement of rotational population lifetimes analogous to the familiar studies of vibrational population relaxation.[22] For systems with optically allowed rotational transitions, such as HCl, one could create a specific nonequilibrium distribution of rotational states with a short (but not ultrashort) IR pulse and then use the absorption of a second IR pulse to watch the populations relax. Examining the dipole–forbidden transitions in H_2 and D_2, though, would require a somewhat more involved approach.

As the particulars of the experiment change, so would the perspectives we would obtain on the relaxation dynamics, but some rough indications of the time scales to be expected might be useful. Just as in vibrational spectroscopy,[22,70] a standard Kubo treatment predicts that the inverse lifetime for a rotational *transition* $l \to l'$ is the sum of

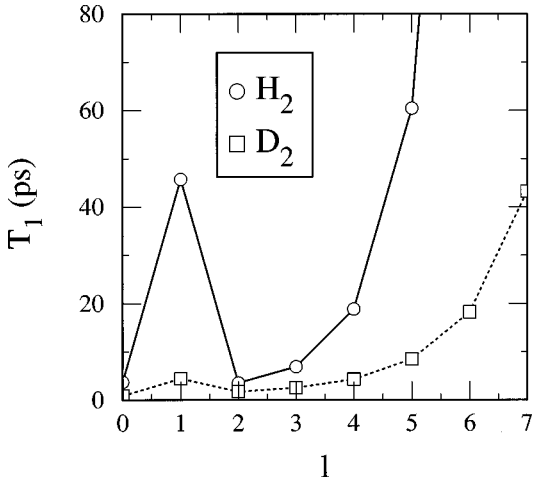

FIG. 8. Predicted population-relaxation lifetimes for individual rotational energy levels (l) of H_2 and D_2 dissolved in dense supercritical Ar (with the lifetimes defined as in Sec. VI). The lines connecting the open symbols are drawn merely to guide the eye.

quantities we can think of as inverse lifetimes for the two rotational levels. In particular, for a rotational energy level l, that inverse lifetime is just the sum of the rate constants for leaving that level[21]

$$1/T_1(l) = \sum_{\substack{l' \\ (l' \neq l)}} k_{l\to l'} = k_{l\to l-2} + k_{l\to l+2} \quad \text{(for our system)}.$$

[By analogy, a master equation treatment of the incoherent population dynamics of a two-state system (0,1) reveals that the value of $1/T_1$ is the sum of $1/T_1(0)=k_{0\to 1}$ and $1/T_1(1)=k_{1\to 0}$.] Lifetimes computed in this fashion (Fig. 8) show an interesting nonmonotonic dependence on rotational state, though one we can understand in some detail: For levels with $l \geqslant 2$, population relaxation can, in principle, occur via both upward ($\Delta l=2$) and downward ($\Delta l=-2$) transitions. However, under our conditions, the downward channel is almost always the faster one for these states (because of detailed-balance considerations, Tables III and IV). Hence, the general increasing trend for $l \geqslant 2$ is simply a direct reflection of the systematic increase in energy gaps with l for $\Delta l=-2$ transitions. By contrast, any excess population in the $l=0$ and $l=1$ levels, can only relax by upward transitions—suggesting that both of these levels should have anomalously long lifetimes. Nonetheless, because of the fivefold increase in degeneracy and the low energy gap for $0\to 2$ transitions, the upward $0\to 2$ transition rate is comparable to the downward $2\to 0$ rate for H_2 (and for D_2 the upward rate is even faster than the downward rate). Hence only the $l=1$ levels end up with anomalous population lifetimes.[71]

Such fine details aside, the more qualitative lessons from Fig. 8 are first, that the population lifetimes of the low-lying rotational states are going to be on the order of picoseconds and second, that D_2 states relax significantly faster than H_2 states. Both of these results have a simple interpretation within the framework of this article: All of the allowed transitions for these low-energy states lie within the *solution's* band, but the D_2 transitions lie deeper within the band. Unfortunately, testing even these basic findings will be difficult until direct lifetime measurements become available. Still, it is interesting to wonder about the implications of this work for more conventional rotational Raman and absorption spectra.[3–11,13,14] The linewidths for such spectra will depend not only on the rates of population relaxation, but also on the rates for pure dephasing, so we will therefore need to defer for a future article any quantitative predictions for such spectra.[21] Such issues notwithstanding, it is tempting to speculate that one of the reasons that DCl peaks are more difficult to see in the far-IR spectra of SF_6 solutions than HCl peaks[3,6,8] is because DCl has smaller transition frequencies and therefore undergoes much more rapid population relaxation. Similarly, one might hazard a guess that the tendency for the HCl peaks to become progressively better resolved as one proceeds from Ar to Kr to Xe solutions[5,6] is due, at least in part, to the progressive shrinkage of the solvent's bandwidth and the concomitant diminishment of population relaxation rates. We look forward to seeing these conjectures studied in greater depth, both experimentally and theoretically.

ACKNOWLEDGMENTS

The authors thank Yuqing Deng and Matthew Zimmt for helpful discussions. This work was supported by NSF Grant No. CHE-9901095.

[1] M. L. Horng, J. A. Gardecki, and M. Maroncelli, J. Phys. Chem. A **101**, 1030 (1997).
[2] D. S. Alavi and D. H. Waldeck, J. Chem. Phys. **94**, 6196 (1991); D. S. Alavi, R. S. Hartman, and D. H. Waldeck, *ibid.* **94**, 4509 (1991); D. S. Alavi and D. H. Waldeck, J. Phys. Chem. **95**, 4848 (1991); R. S. Hartman, D. S. Alavi, and D. H. Waldeck, *ibid.* **95**, 7872 (1991).
[3] G. Birnbaum and W. Ho, Chem. Phys. Lett. **5**, 334 (1970).
[4] L. Galatry and D. Robert, Chem. Phys. Lett. **5**, 120 (1970).
[5] R. M. van Aalst and J. van der Elsken, Chem. Phys. Lett. **13**, 631 (1972); **23**, 198 (1973); D. Frenkel, D. J. Gravesteyn, and J. van der Elsken, *ibid.* **40**, 9 (1976); P. Menger and J. van der Elsken, J. Chem. Phys. **75**, 17 (1981).
[6] G. Birnbaum, Mol. Phys. **25**, 241 (1973).
[7] P. V. Huong, M. Couzi, and M. Perrot, Chem. Phys. Lett. **7**, 189 (1970).
[8] J. P. Perchard, W. F. Murphy, and H. J. Bernstein, Chem. Phys. Lett. **8**, 559 (1971).
[9] S. M. Howdle and V. N. Bagratashvili, Chem. Phys. Lett. **214**, 215 (1993).
[10] D. G. Taylor III and H. L. Strauss, J. Chem. Phys. **90**, 768 (1989); **96**, 3367 (1992); Z. Chen, Y.-Y. Lin, and H. L. Strauss, J. Phys. Chem. B **104**, 3274 (2000).
[11] J. E. Hunter III, D. G. Taylor III, and H. L. Strauss, J. Chem. Phys. **97**, 50 (1992).
[12] H. L. Strauss, Z. Chen, and C.-K. Loong, J. Chem. Phys. **101**, 7177 (1994); Z. Chen, H. L. Strauss, and C.-K. Loong, *ibid.* **110**, 7354 (1999).
[13] L. Xiao and D. F. Coker, J. Chem. Phys. **100**, 8646 (1994).
[14] L. Xiao and D. F. Coker, J. Chem. Phys. **102**, 1107 (1995); H. S. Mei, L. Xiao, and D. F. Coker, *ibid.* **105**, 3938 (1996).
[15] Some of the most intriguing examples of quantized rotation in liquids involve relatively large moment-of-inertia molecules dissolved in superfluid He droplets. We will not be considering such examples in this article. See, for example, J. P. Toennies and A. F. Vilesov, Annu. Rev. Phys. Chem. **49**, 1 (1998).
[16] J. S. Baskin, M. Gupta, M. Chachisvilis, and A. H. Zewail, Chem. Phys. Lett. **275**, 437 (1997); J. S. Baskin, M. Chachisvilis, M. Gupta, and A. H. Zewail, J. Phys. Chem. A **102**, 4158 (1998).
[17] A. V. Storozhev and R. M. Lynden-Bell, Chem. Phys. Lett. **183**, 316 (1991).

[18] S. I. Temkin and W. A. Steele, Chem. Phys. Lett. **215**, 285 (1993); J. Phys. Chem. **100**, 1996 (1996).
[19] S. Gnanakaran, M. Lim, N. Pugliano, M. Volk, and R. M. Hochstrasser, J. Phys.: Condens. Matter **8**, 9201 (1996).
[20] S. Velasco, A. Calvo Hernandez, J. Guemez, and J. Perez, J. Mol. Liq. **39**, 93 (1988); S. Velasco, A. Calvo Hernandez, J. Guemez, J. Perez, and J. A. White, Mol. Phys. **65**, 413 (1988); S. Velasco, J. A. White, and A. Calvo Hernandez, Chem. Phys. **142**, 361 (1990).
[21] J. Jang and R. M. Stratt, J. Chem. Phys. (submitted).
[22] J. C. Owrutsky, D. Raftery, and R. M. Hochstrasser, Annu. Rev. Phys. Chem. **45**, 519 (1994).
[23] R. M. Stratt, in *Ultrafast Infrared and Raman Spectroscopy*, edited by M. D. Fayer (Marcel Dekker, New York, in press).
[24] R. Zwanzig, J. Chem. Phys. **34**, 1931 (1961).
[25] D. W. Oxtoby, Adv. Chem. Phys. **47** (part 2), 487 (1981).
[26] R. M. Whitnell, K. R. Wilson, and J. T. Hynes, J. Phys. Chem. **94**, 8625 (1990); J. Chem. Phys. **96**, 5354 (1992).
[27] M. Tuckerman and B. J. Berne, J. Chem. Phys. **98**, 7301 (1993).
[28] B. J. Berne, M. E. Tuckerman, J. E. Straub, and A. L. R. Bug, J. Chem. Phys. **93**, 5084 (1990).
[29] D. Chandler, *Introduction to Modern Statistical Mechanics* (Oxford University Press, Oxford, 1987), Chap. 8.
[30] M. G. Kurnikova, D. H. Waldeck, and R. D. Coalson, J. Chem. Phys. **105**, 628 (1996); M. Maroncelli, *ibid.* **106**, 1545 (1997).
[31] J. Jang and R. M. Stratt, J. Chem. Phys. **112**, 7524 (2000).
[32] J. Jang and R. M. Stratt, J. Chem. Phys. **112**, 7538 (2000).
[33] G. Goodyear, R. E. Larsen, and R. M. Stratt, Phys. Rev. Lett. **76**, 243 (1996).
[34] G. Goodyear and R. M. Stratt, J. Chem. Phys. **105**, 10050 (1996).
[35] G. Goodyear and R. M. Stratt, J. Chem. Phys. **107**, 3098 (1997).
[36] R. E. Larsen, E. F. David, G. Goodyear, and R. M. Stratt, J. Chem. Phys. **107**, 524 (1997).
[37] B. M. Ladanyi and R. M. Stratt, J. Phys. Chem. A **102**, 1068 (1998).
[38] R. M. Stratt, Acc. Chem. Res. **28**, 201 (1995).
[39] T. Keyes, J. Phys. Chem. A **101**, 2921 (1997).
[40] D. Chandler, in *The Liquid State of Matter: Fluids, Simple and Complex*, edited by E. W. Montroll and J. L. Lebowitz (North-Holland, Amsterdam, 1982).
[41] (a) A. R. Edmonds, *Angular Momentum in Quantum Mechanics*, 2nd ed. (Princeton University Press, Princeton, 1974), pp. 63 and 47; (b) M. Weissbluth, *Atoms and Molecules* (Student edition) (Academic, San Diego, 1978), pp. 31–33.
[42] J. S. Bader and B. J. Berne, J. Chem. Phys. **100**, 8359 (1994); S. A. Egorov and B. J. Berne, *ibid.* **107**, 6050 (1997); S. A. Egorov, E. Rabani, and B. J. Berne, *ibid.* **108**, 1407 (1998); E. Rabani, S. A. Egorov, and B. J. Berne, *ibid.* **109**, 6376 (1998).
[43] J. L. Skinner, J. Chem. Phys. **107**, 8717 (1997); S. A. Egorov and J. L. Skinner, Chem. Phys. Lett. **293**, 469 (1998); S. A. Egorov, K. F. Everitt, and J. L. Skinner, J. Phys. Chem. **103**, 9494 (1999).
[44] P. Schofield, Phys. Rev. Lett. **4**, 239 (1960).
[45] P. A. Egelstaff, Adv. Phys. **11**, 203 (1962).
[46] J. Borysow, M. Moraldi, and L. Frommhold, Mol. Phys. **56**, 913 (1985).
[47] B. J. Berne and G. D. Harp, Adv. Chem. Phys. **17**, 63 (1970).
[48] R. M. Lynden-Bell, in *Molecular Liquids, Dynamics and Interactions*, edited by A. J. Barnes, W. J. Orville-Thomas, and J. Yarwood (Reidel, Dordrecht, 1984).
[49] M. Buchner, B. M. Ladanyi, and R. M. Stratt, J. Chem. Phys. **97**, 8522 (1992).
[50] R. M. Stratt and M. Cho, J. Chem. Phys. **100**, 6700 (1994).
[51] When using INMs to evaluate a correlation function $C(t)$ involving functions of coordinates, it is generally convenient to start with the second derivative function $G(t)=-d^2C/dt^2$, a quantity which can be expressed quite easily in terms of velocity autocorrelation functions for the INM modes. It is then a simple matter to show that $G(t)=k_BT\int_0^\infty d\omega\cos\omega t\rho(\omega)$, with $\rho(\omega)$ the INM influence spectrum for the original correlation function. See Refs. 36 and 50.
[52] B. M. Ladanyi and R. M. Stratt, J. Phys. Chem. **99**, 2502 (1995); **100**, 1266 (1996).
[53] R. E. Larsen and R. M. Stratt, J. Chem. Phys. **110**, 1036 (1999).
[54] D. D. Dlott, in *Laser Spectroscopy in Solids II*, edited by W. Yen (Springer, Berlin, 1989); S. A. Egorov and J. L. Skinner, J. Chem. Phys. **103**, 1533 (1995); **105**, 10153 (1995); **106**, 1034 (1997).
[55] In an atomic fluid, two atoms are considered to be mutual nearest neighbors if each atom in the pair has the other as a nearest neighbor. See R. E. Larsen and R. M. Stratt, Chem. Phys. Lett. **297**, 211 (1998).
[56] T. S. Kalbfleisch, L. D. Ziegler, and T. Keyes, J. Chem. Phys. **105**, 7034 (1996); R. Biswas, S. Bhattacharyya, and B. Bagchi, J. Chem. Phys. **108**, 4963 (1998).
[57] M. F. Pas and B. J. Zwolinski, Mol. Phys. **73**, 471 (1991).
[58] R. J. LeRoy and J. M. Hutson, J. Chem. Phys. **86**, 837 (1987).
[59] M. P. Allen and D. J. Tildesley, *Computer Simulation of Liquids* (Clarendon, Oxford, 1989), pp. 81, 82.
[60] Numerical diagonalization was accomplished by the QL method. W. H. Press, S. A. Teukolsky, W. T. Vetterling, and B. P. Flannery, *Numerical Recipes in Fortran*, 2nd ed. (Cambridge University Press, Cambridge, 1992), Chap. 11.
[61] Numerical fits to the influence spectrum were carried out via the Levenberg–Marquardt method. W. H. Press *et al.* (Ref. 60), Chap. 15.
[62] A. R. Edmonds (Ref. 41), p. 50.
[63] This finding is, in some sense, a refinement of the early suggestions by L. Galatry and D. Robert (Ref. 4) and by D. Frenkel *et al.* (Ref. 5) that the power spectrum of solute–solvent potential ought to govern linewidths of the far IR spectra of HCl solutions. In contrast to the purely electrostatic analysis of Ref. 4, however, we find rotational relaxation to be dominated by the short-ranged part of the solute–solvent potential.
[64] Observations on the center-of-mass translation of H_2 dissolved in ice are consistent with this picture. Inelastic neutron scattering has shown that this translation is exceptionally rapid (Ref. 12) and simulations suggest that the bulk of the rotational dephasing in this system stems from the coupling of this motion to H_2 rotation (Ref. 14). Translation of H_2 in liquid water is discussed by H. S. Mei and D. F. Coker, J. Chem. Phys. **104**, 4755 (1996).
[65] The possibility that vibrational relaxation in liquids might be described in this fashion was discussed by V. M. Kenkre, A. Tokmakoff, and M. D. Fayer, J. Chem. Phys. **101**, 10618 (1994); P. Moore, A. Tokmakoff, T. Keyes, and M. D. Fayer, *ibid.* **103**, 3325 (1995).
[66] J. I. Steinfeld, P. Ruttenberg, G. Millot, G. Fanjoux, and B. Lavorel, J. Phys. Chem. **95**, 9638 (1991).
[67] The parameters shown in the figure were obtained from a chi-square fit to the logarithm of the rotational friction. W. H. Press *et al.* (Ref. 60), Chap. 15.
[68] The spectral densities we are referring to do not include contributions from intramolecular vibration. Even without these intramolecular contributions, though, the spectral range of protic solvents such as water and ethanol are significantly wider than those of polar aprotics such as acetonitrile. See Refs. 19, 26, and M. Cho, G. R. Fleming, S. Saito, I. Ohmine, and R. M. Stratt, J. Chem. Phys. **100**, 6672 (1994).
[69] J. Jang (unpublished).
[70] D. W. Oxtoby, Adv. Chem. Phys. **40**, 1 (1979).
[71] L. Xiao and D. F. Coker (Ref. 13) also find that the $l=1$ level should be special, but their analysis is based on the inhomogeneous broadening one might expect from the rotational sublevels.